Available online at www.sciencedirect.com

ScienceDirect

International Journal of Heat and Mass Transfer 50 (2007) 5087–5098

International Journal of HEAT and MASS TRANSFER

www.elsevier.com/locate/ijhmt

Diffusion creep

A.F. Mills *

Department of Mechanical and Aerospace Engineering, University of California, Los Angeles, CA 90095, USA

Received 19 March 2007; received in revised form 30 June 2007
Available online 1 November 2007

Abstract

Diffusion creep refers to the phenomenon of flow on a surface along which is a concentration gradient. A number of well known mass transfer problems that have usually been analyzed ignoring diffusion creep are revisited, including isobaric and equimolar counterdiffusion, diffusion with one component stationary, and diffusion with surface reactions. The Kramers and Kistemaker model for the creep velocity is used as a benchmark, and the implications of more recent advanced kinetic theory analyses explored. The validity of Graham's law for isobaric counterdiffusion is examined. The resulting phenomenon of diffusiophoresis of Stokesian particles is briefly discussed.

1. Introduction

The no-slip boundary condition of viscous fluid flow does not apply to a gas mixture when there is a concentration gradient along the boundary surface: there is a "diffusion creep" velocity. This phenomenon is analogous to the more well known "thermal creep" on a non-isothermal surface that was first studied by Maxwell [1]. Both phenomena are peculiar in that the kinetic theory of gases is used to describe the molecule–surface interactions that yield the velocities, and yet they can play an important role when continuum equations suffice to describe the bulk flow. Mass transfer problems in which the bulk flow is induced by diffusion only (for example, the Stefan flow of diffusion with one component stationary) are characterized by velocities of the same order as the diffusion creep velocity. The correct analysis of such problems requires use of the diffusion creep velocity boundary condition. In some situations the only flow is that induced by diffusion creep.

For various reasons that will be discussed later, many workers have not been aware of the existence of diffusion creep in continuum flows, or have been mislead by incorrect analyses of the phenomenon. Standard mass transfer texts do not mention diffusion creep, though the monograph on transport in porous catalysts by Jackson [2] does deal with the topic. A number of relevant papers have appeared, mainly in the chemical engineering literature, but did not appear to have much impact. Recently, the kinetic theory community has been active using advanced kinetic theory to predict diffusion creep velocities for various binary gas mixtures, and with different molecular models [3–5].

The purpose of the present study was to revisit a number of well known mass transfer problems that almost always have been analyzed ignoring diffusion creep. The elementary problems of isobaric and equimolar counterdiffusion in a tube are amenable to approximate one-dimensional analytical solution. However, problems such as diffusion with one component stationary, and diffusion with surface reactions, prove to be inherently two-dimensional, and may require numerical solution of the governing equations. Applications of concern include various methods of measuring binary diffusion coefficients, crystal growth in microgravity environments, and diffusiophoresis of non-Brownian particles.

2. The diffusion creep velocity

A formula for the diffusion creep velocity was first derived by Kramers and Kistemayer [6]. Equivalent formulas were obtained subsequently by Jackson [2] and others,

---

* Tel.: +1 310 825 3583; fax: +1 310 206 4830.
E-mail address: amills@seas.ucla.edu

0017-9310/$ - see front matter © 2007 Elsevier Ltd. All rights reserved.
doi:10.1016/j.ijheatmasstransfer.2007.07.023

Nomenclature

c	mean molecular speed; molar concentration
D_{12}	binary diffusion coefficient
d	distance
J	diffusive molar flux
j	diffusive mass flux
Kn	Knudsen number
L	length
M	molecular weight
m	mass fraction
m	molecular mass
N	absolute molar or molecule flux
n	absolute mass flux
P	pressure
R	radius
V	particle velocity
v	velocity
$\hat{v}$	diffusion velocity
x	mole fraction
z	coordinate

Greek symbols

λ	mean free path
μ	viscosity; defined by Eq. (D.2)
ρ	density
σ	slip coefficient

Subscripts

b	bulk
i	species i
w	wall

Superscripts

x	molar
D	diffusiophoresis
KK	Kramers and Kistemaker

though the final results were often obtained using arguably incorrect logic. The model used by these workers is a particularly simple one in which each species is imagined to have an absolute velocity v_i that is the sum of a diffusion velocity and a mass or molar average velocity. Consider a gas mixture adjacent to a z-direction wall. The number flux of species i incident on the wall is $(1/4)N_ic_i$: on an average, each molecule carries transverse momentum m_iv_i to the wall. (All quantities are evaluated at a distance d_i from the wall where on average the molecules of species i had their last collision.) Then the total transverse momentum flux on the wall is

$$\frac{1}{4}\sum_i N_ic_i\mathsf{m}_iv_i = \frac{1}{4}\sum_i \rho_ic_iv_i \tag{1}$$

If we assume perfectly diffuse scattering of the molecules by the wall, Eq. (1) gives the net rate of momentum transfer to the wall. In the absence of a pressure gradient, the net momentum transfer rate to the wall is required to be zero by a force balance; hence

$$\sum_i \rho_ic_iv_i = 0 \tag{2}$$

To proceed on a mass basis we write $v_i = v_\mathrm{w} + \hat{v}_i$ where v_w is the mass average velocity distant d_i from the wall. Now $c_iM_i^{1/2} = \text{const.}$ by equipartion of energy, and $\rho_i = m_i\rho$: substituting and solving for v_w gives

$$v_\mathrm{w} = -\frac{\sum m_iM_i^{-1/2}\hat{v}_i}{\sum m_iM_i^{-1/2}} \tag{3}$$

For a binary mixture $m_1\hat{v}_1 = -D_{12}(\mathrm{d}m_1/\mathrm{d}z) = -m_2\hat{v}_2$ by Fick's law; thus

$$v_\mathrm{w} = \frac{\frac{1}{M_1^{1/2}} - \frac{1}{M_2^{1/2}}}{\frac{m_1}{M_1^{1/2}} + \frac{m_2}{M_2^{1/2}}}D_{12}\frac{\mathrm{d}m_1}{\mathrm{d}z} \tag{4}$$

As an example, consider a mixture of helium (1) and air (2) in a tube of length L, with $m_1 = 1$ at $z = 0$, and $m_1 = 0$ at $z = L$. Then $\mathrm{d}m_1/\mathrm{d}z$ is negative and, since $M_1 < M_2$, v_w is negative. The mass average creep velocity is in the direction of the diffusion of the heavier species, air.

The molar equivalent to Eq. (3) is obtained by writing $v_i = v_\mathrm{w}^* + \hat{v}_i^*$ and $\rho_i = cx_iM_i$ to obtain

$$v_\mathrm{w}^* = -\frac{\sum x_iM_i^{1/2}\hat{v}_i^*}{\sum x_iM_i^{1/2}} \tag{5}$$

For a binary mixture $x_1\hat{v}_1^* = -D_{12}(\mathrm{d}x_1/\mathrm{d}z) = x_2\hat{v}_2^*$, thus

$$v_\mathrm{w}^* = \frac{M_1^{1/2} - M_2^{1/2}}{x_1M_1^{1/2} + x_2M_2^{1/2}}D_{12}\frac{\mathrm{d}x_1}{\mathrm{d}z} \tag{6}$$

Returning to the helium–air example, we see that v_w^* is positive. The molar average creep velocity is in the opposite direction to the mass average value, and is in the direction of diffusion of the lighter species, helium. The physics of the model is clear when the molar based result is examined; there must be a bulk motion of the gas in the direction of helium diffusion to cancel the imbalance in momentum transfer associated with the different molecular weights of the species.

The simple diffusion model used here has many shortcomings. Nevertheless, analyses of equimass and equimolar counterdiffusion, using Eqs. (4) and (6), respectively, yields results in reasonable accord with experiment, particularly when the two molecular weights are very different. Thus these expressions will be used as a benchmark and the implications of more advanced kinetic theory discussed in Appendix A.

3. Isobaric diffusion

3.1. Graham's law

Graham [7] reported experiments on isobaric counterdiffusion of various gas mixtures through a porous plug, and concluded that the molar fluxes were inversely proportional to the square root of molecular weight:

$$\frac{N_1}{N_2} = -\left(\frac{M_2}{M_1}\right)^{1/2} \tag{7}$$

The agreement between experiment and Eq. (7) was excellent. Graham's result was essentially ignored for over a hundred years. Since Graham did not report the average pore size of his Paris plaster plugs, some workers perhaps concluded that the diffusion was in the Knudsen regime ($Kn = \ell/d \gg 1$) for which kinetic theory yields Eq. (7). But the pores in Paris plaster are in fact large, and the continuum limit $Kn \to 0$ applies. For true isobaric one-dimensional diffusion, Newton's second law requires that the mass average velocity be zero: there is no pressure gradient to overcome viscous or inertial forces. The absolute mass flux of species 1 is then

$$n_1 = m_1 \rho v + j_1 = j_1 = \text{const.} \tag{8}$$

and $j_1 = -j_2$ for a binary mixture. Thus

$$n_1 = -n_2 \quad \text{or} \quad N_1 M_1 = -N_2 M_2 \tag{9}$$

and

$$\frac{N_1}{N_2} = -\frac{M_2}{M_1} \tag{10}$$

which contradicts Eq. (7). Eq. (10) applies to an unbounded medium: thus there must be wall effect that causes Eq. (7) to be valid for diffusion in a passage, as noted by Kucherov and Rikenglaz in 1958 [8].

Eq. (7) is now known as Graham's law. Although there is some experimental data to the contrary, nearly all experiments have shown the law to be valid over the whole Knudsen number range from free molecule flow to continuum diffusion. Hoogschagen [9] used a porous plug with 0.8 mm diameter pores to ensure a small Knudsen number. He confirmed Graham's law for He–O_2, N_2–O_2, and CO_2–O_2 mixtures. Evans et al. [10] performed experiments on He–Ar counterdiffusion in large pore graphite (pore radius ~3 μm) at 2 atm total pressure: they found agreement with Graham's law within an experimental error of 4%. The 1962 experimental results of Rothfield [11] are less supportive of Graham's law, particularly for interdiffusion of He and C_4H_{10} or C_5H_{12}. Remick and Geankoplis [12] used a bundle of 644 glass capillaries 0.96 cm long and 3.9 μm diameter. The Knudsen number was varied by varying the absolute pressure from 0.444 to 300.2 mm Hg: above about 100 mm continuum conditions obtained. Graham's law was found to apply over the whole pressure range for He–N_2 interdiffusion. Deviations in the continuum range were no larger than in the free molecule range and could be attributed to experimental error (3–6%).

3.2. Mass based analysis

Consider isobaric, isothermal binary diffusion in a tube of length L. Plug flow with a velocity equal to the mass average diffusion creep velocity v_w, given by Eq. (4) is assumed. The flow is not strictly one-dimensional because v_w is not constant along the tube: however, the Reynolds number is very small ($\ll 1$) so that the velocity profile remains nearly uniform. Also, the small pressure gradient associated with the acceleration of the flow will be ignored. From Eq. (4).

$$v_w = f(m_1) D_{12} \frac{dm_1}{dz}; \quad f(m_1) = \frac{\frac{1}{M_1^{1/2}} - \frac{1}{M_2^{1/2}}}{\frac{m_1}{M_1^{1/2}} + \frac{m_2}{M_2^{1/2}}} \tag{11}$$

The absolute mass flux of species 1 is

$$n_1 = m_1 \rho v_w + j_1 = m_1 \rho v_w - \rho D_{12} \frac{dm_1}{dz} \tag{12}$$

substituting from Eq. (11)

$$n_1 = \rho D_{12} (m_1 f(m_1) - 1) \frac{dm_1}{dz} \tag{13a}$$

Similarly

$$n_2 = \rho D_{12} (m_2 f(m_1) - 1) \frac{dm_1}{dz} \tag{13b}$$

Dividing

$$\frac{n_1}{n_2} = \frac{m_1 f(m_1) - 1}{m_2 f(m_1) + 1} \tag{14}$$

At $z = 0$, $m_1 = 1$, $m_2 = 0$; from Eq. (11)

$$f(m_1) = \frac{\frac{1}{M_1^{1/2}} - \frac{1}{M_2^{1/2}}}{\frac{1}{M_1^{1/2}} - 0} = 1 - \left(\frac{M_1}{M_2}\right)^{1/2}$$

Substituting in Eq. (14)

$$\frac{n_1}{n_2} = -\left(\frac{M_1}{M_2}\right)^{1/2} \tag{15}$$

Since n_1/n_2 is constant by mass species conservation, Eq. (15) applies at all z (and is easily checked at $z = L$). On a molar basis Eq. (15) becomes

$$\frac{N_1}{N_2} = -\left(\frac{M_2}{M_1}\right)^{1/2} \tag{16}$$

which is Graham's law. Thus the simple benchmark model for diffusion creep velocity, Eq. (4), predicts Graham's law exactly, confirming that Graham's law for continuum diffusion is the result of a non-zero mass average velocity at the wall. Recognition of the role played by diffusion creep was slow, partly due to competing derivations of Graham's law using the “dusty gas” model of porous solids, for example [13–15]. However, it can be shown that the dusty gas model cannot, in principle, give Graham’s law, and actually exhibits a singular behavior in the continuum limit.

It is straightforward to continue the mass based analysis to obtain the concentration profiles and species fluxes. However, it is simpler to use a mole based analysis to take advantage of the constant total molar concentration resulting from isobaric and isothermal conditions.

3.3. Mole based analysis

Rather than proceeding as was done for the mass based analysis in Section 3.1, we will follow Scott and Cox [16] and make use of Graham’s law: it has been shown already that Eq. (4), and hence Eq. (6), are consistent with Graham’s law. The absolute molar flux of species 1 is

$$N_1 = x_1(N_1 + N_2) - cD_{12}\frac{\mathrm{d}x_1}{\mathrm{d}z} \tag{17}$$

Hence

$$N_1\left(1 - x_1\left(1 + \frac{N_2}{N_1}\right)\right) = -cD_{12}\frac{\mathrm{d}x_1}{\mathrm{d}z}$$

Defining $\Phi = 1 + N_2/N_1$ and separating variables

$$\frac{\mathrm{d}x_1}{\Phi x_1 - 1} = \frac{N_1\,\mathrm{d}z}{cD_{12}} \tag{18}$$

Integration gives the concentration profile as

$$\frac{\Phi x_1 - 1}{\Phi x_{110} - 1} = \mathrm{e}^{\Phi N_1 z/cD_1 z} \tag{19}$$

where

$$N_1 = \frac{cD_{12}}{\Phi L}\ln\frac{\Phi x_{1,L} - 1}{\Phi x_{1,0} - 1}$$

As a simple illustrative example take $M_1 = 1$, $M_2 = 4$; then $N_2/N_1 = -(1/4)^{1/2} = -1/2$ and $\Phi = -1/2$. Also take $x_{1,0} = 0$, $x_{1,L} = 1$. Substituting in Eqs. (18) and (19)

$$N_1 = 2\ln\frac{1}{2}\,\frac{cD_{12}}{L} = -1.387\frac{cD_{12}}{L} \tag{20}$$

$$x_1 = 2 - 2\mathrm{e}^{\frac{1}{2}N_1 z/cD_{12}} = 2 - 2\mathrm{e}^{-0.6931z/L} \tag{21}$$

Notice that N_1 is 1.387 times the value corresponding to a linear profile. Since v_w^* is negative for $M_1 < M_2$, the shape of the concentration profiles is as shown in Fig. 1. The convective flow augments the diffusion of the lighter species, and is opposite to the diffusion of the heavier species. Note also that Eq. (18) can be obtained by substituting Eq. (6) in Eq. (17) with $cv^* = N_1 + N_2$.

3.4. New results

The good agreement between experiment in the form of Graham’s law and theory in the form of the Kramers and Kistemaker formula for the diffusion creep velocity bears further examination in the light of new advanced kinetic theory models for diffusion creep. These models will be discussed in Appendix A, and the implications for isobaric diffusion explored in Appendix C.

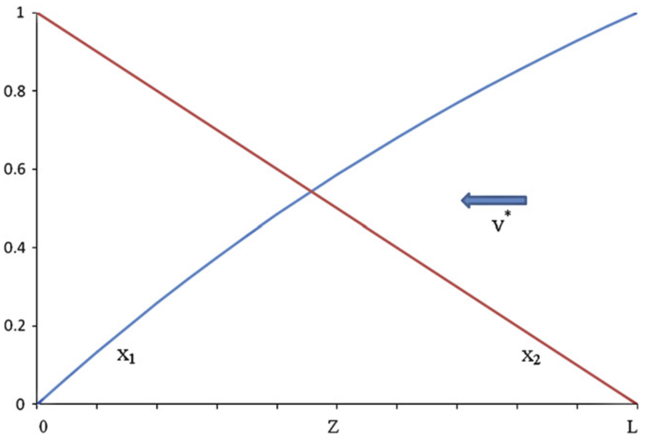

Fig. 1. Concentration profiles for isobaric binary diffusion: $M_1 = 1$, $M_2 = 4$.

4. Equimolar counterdiffusion

The analysis and experiments of Kramers and Kistemaker [6] for equimolar counterdiffusion were major contributions to the subject. More recently, Young and Todd [17] revisited the continuum analysis of equimolar counterdiffusion and developed it in a form that allows satisfactory interpolation with free molecule flow analysis for application in porous solids: the analysis that follows has elements of their development.

Since a one-dimensional diffusion model is sought, we assume plug flow at a velocity equal to the bulk velocity: for laminar flow in a tube

$$v_\mathrm{b} = v_\mathrm{w} + \frac{R^2}{8\mu}\left(-\frac{\mathrm{d}P}{\mathrm{d}x}\right) \tag{22}$$

($v_\mathrm{w} = 0$ for Poiseuille flow). Add the diffusion velocity of species i, $\hat{v}_i$ (which is not a function of r in a one-dimensional model)

$$v_\mathrm{b} + \hat{v}_i = v_\mathrm{w} + \hat{v}_i + \frac{R^2}{8\mu}\left(-\frac{\mathrm{d}P}{\mathrm{d}x}\right)$$

or

$$v_{\mathrm{b}i} = v_{\mathrm{w}i} + \frac{R^2}{8\mu}\left(-\frac{\mathrm{d}P}{\mathrm{d}x}\right) \tag{23}$$

in terms of the species absolute velocity v_i. Now subtract $\hat{v}_i^*$ the diffusion velocity relative to the mole average velocity

$$v_{\mathrm{b}i} - \hat{v}_i^* = v_{\mathrm{w}i} - \hat{v}_i^* + \frac{R^2}{8\mu}\left(-\frac{\mathrm{d}P}{\mathrm{d}x}\right)$$

or

$$v_\mathrm{b}^* = v_\mathrm{w}^* + \frac{R^2}{8\mu}\left(-\frac{\mathrm{d}P}{\mathrm{d}x}\right) \tag{24}$$

We see that an equation of the form of Eq. (22) is valid on a mass or molar basis for one-dimensional flow. Then

$$\frac{R^2}{8\mu}\frac{\mathrm{d}P}{\mathrm{d}z} = -(v_\mathrm{b}^* - v_\mathrm{w}^*) \tag{25}$$

For equimolar counterdiffusion in a binary mixture, $v_\mathrm{b}^* = 0$ and

$$J_1^* = -J_2^* = -cD_{12}\frac{\mathrm{d}x_1}{\mathrm{d}z} = \text{const.} \tag{26}$$

Assume c constant, which implies P and T are constant. Then for a tube length L

$$\frac{\mathrm{d}x_1}{\mathrm{d}z} = -\frac{1}{L} \tag{27}$$

substituting Eqs. (6) and (27) in Eq. (25) gives

$$\frac{\mathrm{d}P}{\mathrm{d}z} = -\frac{8\mu D_{12}}{R^2 L}\frac{M_1^{1/2} - M_2^{1/2}}{x_1 M_1^{1/2} + x_2 M_2^{1/2}} \tag{28}$$

Since $\mu = \mu(x_1)$ and $\mathrm{d}z = -L\,\mathrm{d}x_1$, the variables in Eq. (28) are separable. If following Kramers and Kistemaker we assume μ constant, there is the simple result

$$\Delta P = \frac{4\mu D_{12}}{R^2}\ln\left(\frac{M_1}{M_2}\right) \tag{29}$$

To compare this pressure drop to that if there were no diffusion creep we use the Poiseuille flow result

$$\frac{\mathrm{d}P}{\mathrm{d}z} = -\frac{8\mu}{R^2}v_\mathrm{b} \tag{30}$$

$$\rho v_\mathrm{b} = M_1 N_1 + M_2 N_2 = J_1^*(M_1 - M_2) = \frac{cD_{12}}{L}(M_1 - M_2)$$

$$v_\mathrm{b} = \frac{c}{\rho}\frac{D_{12}}{L}(M_1 - M_2) = \frac{D_{12}}{L}\frac{M_1 - M_2}{M} \tag{31}$$

$$\frac{\mathrm{d}P}{\mathrm{d}z} = -\frac{8\mu D_{12}(M_1 - M_2)}{R^2 L}\int_0^L \frac{1}{x_1 M_1 + x_2 M_2}\mathrm{d}z$$

for μ constant. Again using $\mathrm{d}z = -L\,\mathrm{d}x_1$ gives

$$\frac{\mathrm{d}P}{\mathrm{d}z} = \frac{8\mu D_{12}}{R^2}\ln\frac{M_1}{M_2} \tag{32}$$

which is exactly twice the value obtained with creep.

Kramers and Kistemaker performed experiments on interdiffusion of hydrogen in air in a 0.460 mm diameter, 40 cm long capillary tube. A quasi-steady state was attained corresponding to equimolar counterdiffusion and the pressure differential measured. (Note that, contrary to statements made in many mass transfer texts, a pressure gradient in required for equimolar counterdiffusion since the mass average velocity is non-zero – and is given by Eq. (28).) They found that the measured pressure drop was 66% of the Poiseuille flow result, Eq. (32) and 32% higher than the expected value given by numerical integration of Eq. (28) to account for the dependence of viscosity on composition. Kramers and Kistemaker recommend further experiments to evaluate the validity of Eq. (28). However, another possibility is that their model for diffusion creep velocity is not completely adequate. Recent advanced kinetic theory models of diffusion creep are discussed in Appendix A, and their application to equimolar counterdiffusion in Appendix B.

5. Diffusion with one component stationary

Analyses of diffusion with one component stationary are presented in standard texts, sometimes in connection with the Stefan tube used to measure diffusion coefficients, e.g. [18], but also in connection with heatpipes, e.g. [19]. These analyses are one-dimensional and are essentially exact for an unbounded medium. When applied to a gas mixture confined in a duct, the assumption of plug flow is made. Some years ago there was concern about the impact of violating the usual non-slip boundary condition of fluid mechanics. An exact numerical solution for a cylindrical tube was obtained by McDonald et al. [20], who showed that even at very high mass transfer rates the error incurred in using the 1D analysis was less than 5%. Unaware of this work, related numerical studies were made by Meyer and Kostin [21], and Markham and Rosenberger [22]. At their lower rates of mass transfer, the latter authors found no error in one-dimensional predictions to within the 1% accuracy of the numerical results.

Whitaker [23] pointed out that the numerical studies ignored the presence of diffusion creep, but did not take the matter further. To examine the possible effect of the creep velocity we will consider a one-dimensional model with species 2 stationary. Then the absolute mass fluxes of the two components are

$$n_1 = m_1\rho v_\mathrm{b} - \rho D_{12}\frac{\mathrm{d}m_1}{\mathrm{d}z} \tag{33}$$

$$n_2 = m_2\rho v_\mathrm{b} - \rho D_{12}\frac{\mathrm{d}m_2}{\mathrm{d}z} \tag{34}$$

Since $n_1 + n_2 = n_1 = \rho v_\mathrm{b}$, Eq. (33) gives the bulk velocity as

$$v_\mathrm{b} = -\frac{1}{1 - m_1}D_{12}\frac{\mathrm{d}m_1}{\mathrm{d}z} \tag{35}$$

From Eq. (4) the diffusion creep velocity with $\beta = (M_1/M_2)^{1/2}$ is

$$v_\mathrm{w} = \frac{1 - \beta}{\beta + m_1(1 - \beta)}D_{12}\frac{\mathrm{d}m_1}{\mathrm{d}z} \tag{36}$$

The ratio of the creep velocity to the bulk velocity is then

$$\frac{v_\mathrm{w}}{v_\mathrm{b}} = -\frac{(1 - m_1)(1 - \beta)}{\beta + m_1(1 - \beta)} \tag{37}$$

The water vapor–air system has been of much interest in connection with diffusion with one component stationary. Then $\beta = (18/29)^{1/2} = 0.79$–$0.8$ and Eq. (37) becomes

$$\frac{v_\mathrm{w}}{v_\mathrm{b}} = -\frac{1 - m_1}{4 + m_1}$$

Table 1 shows the result. At most v_w is 25% of v_b, and is in the opposite direction to the bulk velocity. Since the

Table 1
The ratio of creep velocity to bulk velocity for water vapor diffusing through stationary air

m_1	0.01	0.1	0.5	0.9	0.99
$v_\mathrm{w}/v_\mathrm{b}$	−0.25	−0.22	−0.11	−0.02	−0.002

numerical studies that assumed $v_\mathrm{w} = 0$ showed negligible effect on the mass transfer rate, these relatively small negative values of v_w also should not have significant effect. If the computer codes used to generate the results given in Refs. [20,22] are still available it would be a relatively simple task to modify the boundary conditions and recalculate results, though such an exercise would be of marginal value. The two-dimensional character of the real flow has but a small effect on the mass transfer rate. Accounting for creep velocity will give somewhat higher axial pressure gradients, but the gradients are negligibly small.

6. Diffusion in a porous catalyst

Diffusion with chemical reaction is relevant to many chemical engineering processes: diffusion with chemical reaction in porous catalyst has received considerable attention over the years. We will consider pores of diameter large enough to ensure continuum conditions, and a simple model problem for which the reaction takes place at the end of a pore, as shown in Fig. 2a. The reaction is the catalytic dissociation of hydrogen, $H_2 \rightarrow 2H$ at $z = 0$. In a one-dimensional model the absolute fluxes of species 1(H) and species 2(H_2) in a binary mixture are

$$n_1 = m_1 \rho v_\mathrm{b} + j_1 \tag{38a}$$

$$n_2 = m_2 \rho v_\mathrm{b} + j_2 \tag{38b}$$

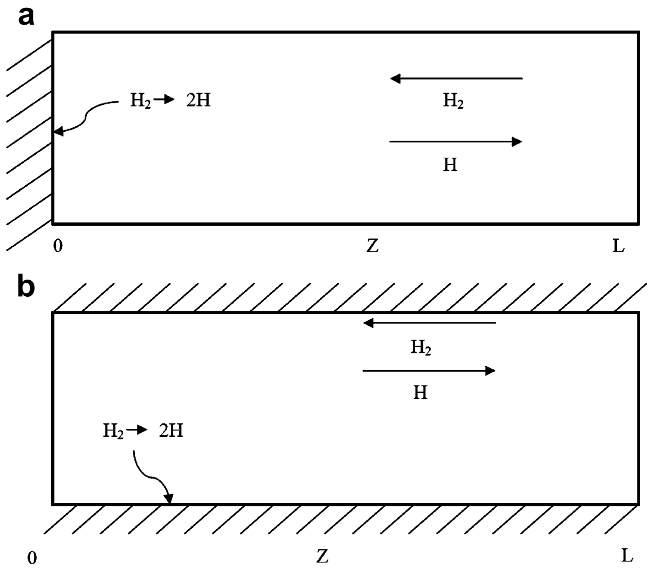

Fig. 2. Diffusion in a pore with a dissociation reaction on the (a) end wall; (b) side wall.

But what is the appropriate value of v_b in one-dimensional analysis? Adding Eqs. (38a) and (38b) given

$$n_1 + n_2 = \rho v_\mathrm{b} \tag{39}$$

at $z = 0$; $v_\mathrm{b} = 0$ for a catalytic reaction, so

$$v_\mathrm{b} = v_{\mathrm{b}|0} = 0 \tag{40}$$

On the other hand, the diffusion creep velocity from Eq. (4) with $\beta = (M_1/M_2)^{1/2}$

$$v_\mathrm{w} = \frac{1-\beta}{\beta + m_1(1-\beta)} D_{12} \frac{\mathrm{d}m_1}{\mathrm{d}z} \tag{41}$$

and is negative ($\beta < 1$, $\mathrm{d}m/\mathrm{d}z$ negative). In the case of equimass counterdiffusion dealt with in Section 3, the bulk velocity could be approximated by the slip velocity. This case is also equimass counterdiffusion, but now the reaction at $z = 0$, requires $v_\mathrm{b} = 0$. The correct solution must be two-dimensional involving a flow towards $z = 0$ near the walls, and away from $z = 0$ in the core. To obtain some idea of relative magnitudes we can compare ρv_w to the diffusion flux j_i

$$j_1 = -\rho D_{12} \frac{\mathrm{d}m_1}{\mathrm{d}z} \tag{42}$$

$$\frac{\rho v_\mathrm{w}}{j_1} = -\frac{1-\beta}{\beta + m_1(1-\beta)} \tag{43}$$

For the $H_2 \rightarrow 2H$ problem, $\beta = 0.707$

$$-\frac{\rho v_\mathrm{w}}{j_1} = \frac{1}{2.41 + m_1} \tag{44}$$

Table 2 shows that the ratio varies from 0.414 at $z = 0$, to 0.293 at $z = L$, for m_1 varying from 0 to 1. As for diffusion with one component stationary, there should be little error in mass transfer rates given by a one-dimensional model with $v_\mathrm{b} = v_\mathrm{w} = 0$. However, it would be useful to obtain two-dimensional solutions to support this conjecture.

A problem more pertinent to porous catalysts is a locally rate controlled reaction occurring on the side walls of a pore, as shown in Fig. 2b. The classical analysis of this problem assumes one-dimensional diffusion with the reaction expressed in terms of the bulk concentration. There is no change to Eq. (1) since the desorption of the product is surely diffuse. As for the previous situations considered, the two-dimensional character of the flow should have little impact on mass transfer results. More importantly, it would be inappropriate to include the effect of diffusion creep without considering other complicating factors such as temperature gradients causing thermal creep, and pressure differentials across the pellet causing a bulk flow.

Table 2
The ratio of creep convective flux to diffusion flux for $2H \rightarrow H_2$ in a pore

m_1	0.01	0.1	0.5	0.9	1.0
$-\rho v_\mathrm{w}/j_1$	0.414	0.396	0.344	0.302	0.293

7. Microgravity crystal growth

Diffusion and thermal creep are pertinent to crystal growth experiments at microgravity in closed ampoules. As was the case for isobaric diffusion in Section 3, a convective flow is produced by the creep velocities (if the no-slip condition were valid, there would be no flow: the gas mixture would be stationary [24]). Two-dimensional solutions for the isothermal case have been obtained by Papadopoulos and Rosner [25] using a direct simulation Monte Carlo method to solve the governing Boltzmann equation for nominal Knudsen numbers in the range 0.5–0.2 (the nominal Knudsen number was defined in terms of the length of the enclosure). It was found that end effects at $Kn = 0.5$ have a marked effect on the creep velocity, as might be expected. Calculations were performed for binary gas mixtures with species of equal molecular weights but different accommodation coefficients (see Appendix A), as well as for unequal molecular weights and unity accommodation coefficients. A flow circulation was found with the core velocity in the opposite direction to the wall creep velocity. The convective flow along the end wall, where crystal growth occurs, could cause undesirable non-uniformities. Further work is required to investigate this possibility.

8. Closing comment

In the review process for this manuscript, a request was made for comments on the relation between the present work and that of Kerkhof et al. [26–28]. The present work is a demonstration that various well known mass transfer problems can be solved using the conventional conservation equations for species, and if necessary, momentum, provided no-slip boundary conditions are replaced by diffusion creep velocity boundary conditions. On the other hand, Kerkhof and Geboers [27] argued that these conservation equations could not be used: however, this assertion was based on the concomitant use of the no-slip boundary condition. In an earlier paper [26] they dismissed the derivation of a diffusion creep velocity by Kramers and Kistemaker [6], on the grounds that “no clear indication of velocity profiles was taken into account” and subsequently ignored diffusion creep. Instead they chose to follow an approach, originally suggested by Whitaker for the Stefan tube [23], in which the species conservation equations are replaced by species momentum equations. Models for the species interaction terms are then introduced to yield, for example, Eq. (44) of Kerkhof and Geboers [28]. These species momentum equations have an unfortunate singularity as species concentration goes to zero that is simply ignored. Mills [29] discusses the relevance of the singularity to the physical meaning of a species velocity. Of more concern is that the final equations violate Fick’s law for binary diffusion, or more generally, the Maxwell–Stefan equations obtained from solving the Boltzmann equation for transport of a mass species, given as Eqs. (7.4)–(48) of Hirschfelder et al. [30]. In solving these equations for diffusion in a pore or capillary, they introduce Maxwell’s velocity slip formula for slip flow applied to each species separately, and rewrite the slip coefficient in terms of the Knudsen diffusion coefficient. The result is essentially an interpolation formula between slip flow and free molecule flow. Graham’s law is obtained, but in much the same way the discredited dusty gas model also yields Graham’s law for small but non-zero Knudsen numbers. An interpolation formula that correctly gives the continuum limit has recently been proposed by Young and Todd [17], based on an analysis that appears to be free of the difficulties inherent in the dusty gas and Kerkhof approaches.

Appendix A. The diffusion creep velocity

As was stated in Section 2, a formula for the diffusion creep velocity was first derived by Kramers and Kistemaker, using a simple flow model of diffusion [6]. The mass average creep velocity in terms of mole fraction gradient is

$$v_{\mathrm{w}} = \frac{\left(\frac{M_2}{M}\right)\left(\frac{M_1}{M_2}\right)^{1/2} - \left(\frac{M_1}{M}\right)}{x_1\left(\frac{M_1}{M_2}\right)^{1/2} + x_2} D_{12}\frac{\mathrm{d}x_1}{\mathrm{d}z} \tag{A.1}$$

This result assumes diffuse reflection of molecules, that is, an accommodation coefficient α of unity. Subsequently authors [17,31] have proposed formulas that allow $\alpha_1 \neq \alpha_2 < 1$. A fraction $(1 - \alpha)$ is reflected specularly, while fraction α is either reflected diffusely or desorbed diffusely. The motivation for allowing $\alpha_1 \neq \alpha_2$ was to have a model that would predict a non-zero creep velocity for two species of equal molecular weight. Experiments [32] have shown a non-zero creep velocity for mixtures of C_2H_2–N_2 and CO_2–C_3H_8. However, there has been no direct experimental confirmation of the improved models because necessary data for the relevant accommodation coefficients have not been available. Thus we will restrict attention to results for diffuse reflection.

There have been very many determinations of the diffusion creep velocity using advanced kinetic theory. The studies vary with different techniques used to solve the Boltzmann equation, and different models for molecule interaction have been used. All are one-dimensional. If a Knudsen number is defined in terms of a characteristic length of the surface, the results are only valid for small Knudsen numbers: otherwise there are significant end effects [25]. The important advances over the simplistic model of Kramers and Kistemaker are (i) variables vary continuously normal to the surface – there is no Knudsen layer, and (ii) realistic models of molecule interaction have been incorporated. Evaluation of these kinetic theory results is made difficult by the use of various forms for the creep velocity and imprecise definitions. In line with many of the studies we will write

$$v_{\mathrm{w}} = \sigma D_{12}\frac{\mathrm{d}x_1}{\mathrm{d}z} \tag{A.2}$$

where σ is a dimensionless "diffusion" or "concentration" creep coefficient. The Kramers and Kistemaker result is

$$\sigma^{\mathrm{KK}} = \frac{\left(\frac{M_2}{M}\right)\left(\frac{M_1}{M_2}\right)^{1/2} - \left(\frac{M_1}{M}\right)}{x_1\left(\frac{M_1}{M_2}\right)^{1/2} + x_2} \tag{A.3}$$

The only more advanced kinetic theory result that is in algebraic form was obtained by Loyalka [33]. But in more recent papers Loyalka and coworkers present new analyses that yield numerical results: these presumably supercede the 1971 formula, which will not be discussed further. Ivchenko et al. [3] obtained numerical results for various gas mixtures using the Lennard-Jones potential model. Their results are given in the form of graphs of σ versus the mole fraction of species 1. In a more recent paper [34], the same authors explored the consequences of using first and second order Chapman–Enskog approximations, and the rigid sphere versus Lennard-Jones potential models. Using the second approximation had only a small effect when using the Lennard-Jones model, but a somewhat larger effect when using the rigid sphere model. For example, consider H_2–N_2 mixtures with $x_1 = 0.01$: for the Lennard-Jones model the change in σ was 3.3% while for the rigid sphere model it was 8.1%.

Sharipov and Kalempa [4] give numerical results for three mixtures of noble gases using both a rigid sphere model and a "realistic" potential model obtained from experimental data for the transport coefficients of mixture. The Boltzmann equation was solved using the approximate McCormack model. Takata and coworkers [5,35] also used advanced kinetic theory to calculate diffusion creep velocities. Results are presented for a rigid sphere model and molecular weight ratios ranging from 2 to 10. The exact Boltzmann equation was used. To evaluate the adequacy of the McCormack model, Sharipov and Kalempa made comparisons with Takata's results and showed agreement to within 5%. Thus detailed comparisons will not be made with Takata's results here.

In contrast to the kinetic theory approach, Brenner and Bielenberg [36,37] have proposed an interesting continuum model for diffusion creep. It has its genesis in a hypothesis that the correct velocity to use in the stress terms of the Navier–Stokes equation for a variable density fluid is the volume average value, rather than the mass average value [36]. As a consequence it is proposed that the no-slip condition at a wall should specify a zero volume average velocity. The resulting value of σ is the simple form

$$\sigma = \frac{M_2 - M_1}{M} \tag{A.4}$$

Follow the same procedure used to derive Eq. (10) for isobaric diffusion there results:

$$\frac{N_1}{N_2} = -\frac{M_2}{M_1} \tag{A.5}$$

which is in serious disagreement with Graham's law.

To make comparisons of the various results for σ we will first consider helium–argon mixtures because a number of authors have obtained results for this system: also, the large molecular weight ratio $M_2/M_1 = 10$ suggests that simpler models will more likely work well. Table A.1 shows a comparison for σ as a function of composition. The approximate values shown for Ivchenko et al. are due to the need to use a graph rather than numerical results. It is seen that the kinetic theory results all agree reasonably well, with the simple Kramers and Kistemaker model doing remarkably well. By chance, it agrees better (±10%) with the realistic potential models rather than the rigid sphere model. In contrast, the continuum model of Brenner and Bielenberg is in sharp disagreement with the kinetic theory results. Table A.2 shows a comparison for neon-argon mixtures. Again the σ values for the realistic potential models of Sharipov and Kalempa and Ivchenko et al. are in very good agreement. The simple Kramers and Kistemaker model gives values that are too low by 18–22%. Surprisingly though, the Kramers and Kistemaker model gives results in quite good agreement with the rigid sphere results of Sharipov and Kalempa. It is seen that when the molecular weights are closer ($M_2/M_1 = 2$) a realistic potential model is required for accurate results. Also, again the Brenner and Bielenberg model is in sharp disagreement.

The air–water vapor system is of great interest in connection with both technology and atmospheric physics. The movement of small non-Brownian droplets of water in air due to diffusiophoresis is often of concern, and as shown in Appendix D, the diffusiophoretic velocity of such droplets is simply the negative of the diffusion creep velocity. Ivchenko et al. [34] present results for air–H_2O mixtures in graphical form. Table A.3 shows a comparison with values obtained from the Kramers and Kistemaker formulas. The latter values are seen to be consistently too large, the discrepancy varying from 30% to 41%. Again the Brenner and Bielenberg formula is in sharp disagreement.

Table A.1
The diffusion creep coefficient for He–Ar mixtures; species 1 is helium

x_1	σ				
	1	2	3	4	5
0.01	0.22	0.252	0.194	0.2	0.908
0.1	0.255	0.285	0.228	0.3	0.989
0.5	0.72	0.629	0.534	0.6	1.64
0.9	2.88	2.91	4.03	2.9	4.74
0.99	6.14	5.94	5.03	6	8.25

Values from various authors: (1) Kramers and Kistemaker [6]; (2) Sharipov and Kalempa, realistic potential model [4]; (3) Sharipov and Kalempa, rigid sphere model; (4) Ivchenko, Loyalka and Tompson, Lennard-Jones model [3]; (5) Brenner and Bielenberg [36,37].

Table A.2
The diffusion creep coefficient for Ne–Ar mixtures; species 1 is neon

x_1	σ				
	1	2	3	4	5
0.01	0.207	0.27	0.22	0.25	0.50
0.1	0.223	0.30	0.23	0.29	0.53
0.5	0.319	0.394	0.313	0.381	0.66
0.9	0.501	0.571	0.459	0.556	0.91
0.99	0.564	0.689	0.551	0.671	0.97

Values from various authors: (1) Kramers and Kistemaker [6]; (2) Sharipov and Kalempa, realistic potential model [4]; (3) Sharipov and Kalempa, rigid sphere model; (4) Ivchenko, Loyalka and Tompson, Lennard-Jones model [3]; (5) Brenner and Bielenberg [36,37].

Table A.3
The diffusion creep coefficient for air–H_2O mixtures; species 1 is air

x_1	$-\sigma$		
	1	2	3
0.01	0.34	0.24	0.61
0.1	0.31	0.22	0.58
0.5	0.23	0.17	0.47
0.9	0.18	0.14	0.39
0.99	0.17	0.13	0.38

Values from various authors: (1) Kramers and Kistemaker [6]; (2) Ivchenko, Loyalka and Tompson, Lennard-Jones model [3]; (3) Brenner and Bielenberg [36,37].

Appendix B. Equimolar counterdiffusion revisited

In Section 4, equimolar counterdiffusion was analyzed using the Kramers and Kistemaker model for the diffusion creep velocity. These authors also did experiments with hydrogen–air mixtures to determine the pressure gradient associated with equimolar counterdiffusion. The pressure gradient is required to overcome wall shear since the mass average velocity is not zero. As noted in Section 4, their measured values of pressure gradient were 32% higher than the expected value, a result they could not explain. A possible reason is that their diffusion creep velocity model is inadequate. Table B.1 shows a comparison of their σ values with values given by Ivchenko et al. [3] for N_2–H_2 mixtures. It is seen that their values are consistently higher than the results using the Lennard-Jones potential model, the discrepancy varying from 13% to 30%. The values in Table B.1 are approximate since they were read off a graph.

Table B.1
Diffusion creep coefficient σ for N_2–H_2 mixtures

X_{N_2}	$-\sigma$	
	1	2
0	10.22	
0.05	5.46	4.9
0.25	1.43	1.2
0.5	0.327	0.5
0.75	0.312	0.25
1.0	0.196	0.15

(1) Kramers and Kistemaker [6]. (2) Ivchenko et al. [3]. The latter values are obtained from a graph presented in Ref. [3].

In order to calculate the pressure gradient we need values of v_w^* in terms of mole fraction to substitute in Eq. (25), whereas Eq. (A.2) defines σ in terms of v_w. The relation between v^* and v is

$$v^* = v + D_{12}\frac{1}{M}\frac{dM}{dz} \tag{B.1}$$

Substituting for v from Eq. (A.2)

$$v_w^* = \sigma D_{12}\frac{dx_1}{dz} + D_{12}\frac{1}{M}\frac{dM}{dz} \tag{B.2}$$

or

$$v_w^* = \left(\sigma + \frac{M_1 - M_2}{x_1(M_1 - M_2) + M_2}\right)D_{12}\frac{dx_1}{dz} \tag{B.3}$$

Substituting in Eq. (25) and using Eq. (27)

$$\frac{dP}{dz} = -\frac{8\mu(x_1)D_{12}}{R^2L}\left[\sigma(x_1) + \frac{M_1 - M_2}{x_1(M_1 - M_2) + M_2}\right] \tag{B.4}$$

The σ values in column 3 of Table B.1 were curve fitted as $\sigma(x_1)$ and substituted in Eq. (B.4). Also, the viscosity of the mixture was calculated using the Lennard-Jones potential model and Wilke mixture rule using the software GASMIX [38], and curve fitted as $\mu(x_1)$. Numerical integration for $x_1(0) = 0$, $x_1(L) = 1$ gives the pressure drop as

$$\Delta P = 4.75\frac{\bar{\mu}D_{12}}{R^2}\ln\frac{M_1}{M_2}\ \text{Pa/m} \tag{B.5}$$

where $\bar{\mu}$ is taken as $\mu(x_1 = 0.5)$ for convenience. To obtain Eq. (B.5) all properties were calculated for a N_2–H_2 mixture. In a second calculation $\sigma(x_1)$ was taken from column 2 of Table B.1 (Kramers and Kistemaker) to give a coefficient of 4.19.

Thus the use of the Ivchenko et al. σ values gives an increase in pressure drop of 11.3% over the variable viscosity Kramers and Kistemaker result, which partially explains the 32% higher value obtained in their experiments.

Appendix C. Equimass counterdiffusion revisited

In Appendix B, it was found that numerical results for the diffusion creep coefficient σ could be incorporated in a one-dimensional analysis of equimolar counterdiffusion to obtain estimates of the pressure drop that are an improvement over the result obtained by Kramers and Kistemaker. In the case of equimass counterdiffusion, associated with a zero pressure gradient, the situation is more complicated. Eq. (14) gives

$$\frac{n_1}{n_2} = \frac{m_1 f(m_1) - 1}{m_2 f(m_2) + 1} \tag{C.1}$$

where from the Kramers and Kistemaker result

$$f(m_1) = \frac{\frac{1}{M_1^{1/2}} - \frac{1}{M_2^{1/2}}}{\frac{m_1}{M_1^{1/2}} + \frac{m_2}{M_2^{1/2}}} \tag{C.2}$$

In a one-dimensional analysis n_1/n_2 is a constant. Substituting Eq. (C.2) in Eq. (C.1) and evaluating at $z = 0$ ($m_1 = 1$, $m_2 = 0$) and $z = L$ ($m_1 = 0$, $m_2 = 1$) gives in both cases

$$\frac{n_1}{n_2} = -\left(\frac{M_2}{M_1}\right)^{1/2} \tag{C.3}$$

which is Graham's law.

Eq. (C.1) can be solved for $f(m_1)$ in terms of $C = n_1/n_2$ as

$$f(m_1) = \frac{C+1}{m_1 - C(1-m_1)} \tag{C.4}$$

The use of Eq. (C.2) for $f(m_1)$ with, for example, $M_1 = 1$, $M_2 = 4$, shows that $C = -1/2$ satisfies Eq. (C.4), as expected from Graham's law. But, if advanced kinetic theory results for the diffusion creep coefficient are used for $f(m_1)$, it is found that Eq. (C.4) is not exactly satisfied, which suggests that a simple one-dimensional solution is not possible. Note also that, since v_w is not constant, there is a small pressure gradient associated with acceleration which contradicts the isobaric diffusion assumption. It does not appear profitable to attempt further analysis of the isobaric diffusion case.

Appendix D. Diffusiophoresis

An important manifestation of diffusion creep is the diffusiophoresis of large (non-Brownian or Stokesian) particles, that is, particle movement due to species concentration gradients in the host gas mixture. It is analogous to thermophoresis, which is the movement of particles down a temperature gradient. Indeed, Maxwell developed his theory of thermal creep in order to explain the phenomenon of thermophoresis [1]. A useful review of early work on diffusiophoresis and thermophoresis was given by Waldmann and Schmitt [39]. As was the case for diffusion creep (and perhaps even more so!), particular care must be taken to use consistent mass or molar formulations.

Although our concern here is large particles, it is helpful to first consider small Brownian particles. Waldmann and Schmitt [39] give the diffusiophoretic velocity for small spherical particles ($d_p \ll \ell$) as

$$V^D = \sum_i \mu_i \mathbf{v}_i \tag{D.1}$$

For equal accommodation coefficients

$$\mu_i = \frac{x_i M_i^{1/2}}{\sum_k x_k M_k^{1/2}} \tag{D.2}$$

Substituting

$$\mathbf{v}_i = \mathbf{v} + \hat{\mathbf{v}}_i = \mathbf{v}^* + \hat{\mathbf{v}}_i^* \tag{D.3}$$

in Eq. (D.1) gives

$$V^D = \mathbf{v} + \sum_i \mu_i \hat{\mathbf{v}}_i = \mathbf{v}^* + \sum_i \mu_i \hat{\mathbf{v}}_i^* \tag{D.4}$$

We now consider one-dimensional diffusion in a binary mixture. On a molar basis

$$x_1 \hat{v}_1^* = -x_2 \hat{v}_2^* = -D_{12}\frac{\mathrm{d}x_1}{\mathrm{d}z} \tag{D.5}$$

Substituting in Eq. (D.4) and using Eq. (D.2)

$$V^D - v^* = -\frac{M_1^{1/2} - M_2^{1/2}}{x_1 M_1^{1/2} + x_2 M_2^{1/2}} D_{12}\frac{\mathrm{d}x_1}{\mathrm{d}z} \tag{D.6}$$

On a mass basis

$$m_1 \hat{v}_1 = -m_2 \hat{v}_2 = -D_{12}\frac{\mathrm{d}m_1}{\mathrm{d}z} \tag{D.7}$$

$$V^D - v = \frac{\frac{x_1}{m_1} M_1^{1/2} - \frac{x_2}{m_2} M_2^{1/2}}{x_1 M_1^{1/2} + x_2 M_2^{1/2}} D_{12}\frac{\mathrm{d}m_1}{\mathrm{d}z} \tag{D.8}$$

Using $x_i = (m_i/M_i)/\sum m_\mathrm{k} M_\mathrm{k}$, Eq. (D.8) can be obtained in terms of mass quantities only as

$$V^D - v = -\frac{\frac{1}{M_1^{1/2}} - \frac{1}{M_2^{1/2}}}{\frac{m_1}{M_1^{1/2}} + \frac{m_2}{M_2^{1/2}}} D_{12}\frac{\mathrm{d}m_1}{\mathrm{d}z} \tag{D.9}$$

Particle transport in a binary mixture with one component stationary is often encountered, e.g. for condensation of a vapor and a noncondensable gas. In this situation it is useful to have an expression for the absolute particle velocity V^D. From Eqs. (D.1) and (D.2) for a binary mixture with $\mathbf{v}_2 = 0$ and $a_1 = a_2$

$$V^D = \mu_1 v_1 = \frac{x_1 M_1^{1/2}}{x_1 M_1^{1/2} + x_2 M_2^{1/2}} \mathbf{v}_1 \tag{D.10}$$

that is, the particle velocity is in the same direction as the velocity of the non-stationary species. Clearly, the stationary species cannot cause the particle to move. Now considering one-dimensional diffusion and $v_2 = 0$

$$v_1 = -\frac{1}{x_1(1-x_1)} D_{12}\frac{\mathrm{d}x_1}{\mathrm{d}z}$$

thus

$$V^D = -\frac{M_1^{1/2}}{x_1 M_1^{1/2} + x_2 M_2^{1/2}} \frac{1}{x_2}\frac{\mathrm{d}x_1}{\mathrm{d}z} \tag{D.11}$$

Eqs. (D.8), (D.9), and (D.11) for small particles were derived using a kinetic theory model since the mean free path in the gas was much larger than the particle size (Kn_p large). For large (non-Brownian particles) $Kn_\mathrm{p} \to 0$. Waldmann and Schmitt [39] consider a spherical particle at rest in an isothermal binary mixture and determine the force acting on the particle due to diffusion creep. This force is then equated to the continuum model Stokes drag to give the velocity that an otherwise free particle will move, which is the diffusiophoretic velocity. Using the Kramers and Kistemaker model for the diffusion creep velocity they obtained results identical to those obtained for small particles! Furthermore, they showed that the result for large particles was independent of particle shape. Thus, Eqs. (D.8), (D.5) and (D.11) should apply to particles of any size. Since the Kramers and Kistemaker diffusion creep model is a kinetic theory model, albeit applied to a Knudsen layer adjacent to the surface, it is perhaps not unexpected that V_D is independent of particle size and particle Knudsen number.

Waldmann and Schmitt [39] evaluated these equations for large particles using various experimental data, and concluded that the agreement was poor. Thus they recommend an empirical alternative to Eq. (D.6)

$$V^D - v^* = -\left(0.95\frac{M_1 - M_2}{M_1 + M_2} - 1.05\frac{d_1 - d_2}{d_1 + d_2}\right)D_{12}\frac{\mathrm{d}x_1}{\mathrm{d}z} \tag{D.12}$$

where d_1 and d_2 are the molecular diameters of the two gas components. However, it may not be prudent to accept their suggestion at face value because the experimental measurement of diffusiophoretic velocities is very difficult. Furthermore, often sufficient details are available to perform satisfactory error analyses of the experiments.

If we accept that Eq. (D.9) is valid for large particles, there is an interesting consequence for isobaric diffusion in a duct. As shown in Section 3.2, the mass average velocity of the gas mixture is equal to the diffusion creep velocity given by Eq. (4). Substituting in Eq. (D.9) shows that $V^D = 0$! That is, free particles in the gas mixture will be stationary. As a corollary, this observation indicates that care must be taken to identify possible diffusion creep induced flows in experiments designed to determine diffusiophoretic particle velocities.

Diffusiophoresis in the continuum limit, $Kn_\mathrm{p} \to 0$ has recently received the attention of Brenner and Bielenberg [36,37]. Their approach is a purely continuum model with no utilization of kinetic theory. The diffusion creep velocity given by their analysis is discussed in Appendix A, where it is shown that it does not yield Graham's law. The resulting diffusiophoretic velocity is

$$V^D - v^* = -\frac{M_1 - M_2}{x_1M_1 + x_2M_2}D_{12}\frac{\mathrm{d}x_1}{\mathrm{d}z} \tag{D.13}$$

A comparison of the Brenner and Bielenberg diffusion creep velocity, namely

$$v^* = \frac{M_1 - M_2}{x_1M_1 + x_2M_2}D_{12}\frac{\mathrm{d}x_1}{\mathrm{d}z} \tag{D.14}$$

with advanced kinetic theory results is given in Appendix A. Since the empirical Eq. (D.12) has a coefficient independent of composition, it is pointless to compare it with Eq. (D.13) for which there is a marked composition dependence.

References

[1] J.C. Maxwell, On stresses in rarified gases arising from inequalities of temperature, Philos. Trans. Roy. Soc. London 170 (1879) 231.

[2] R. Jackson, Transport in Porous Catalysts, Elsevier, Amsterdam, The Netherlands, 1977.

[3] I.N. Ivchenko, S.K. Loyalka, R.V. Tompson, Slip coefficients for binary mixtures, J. Vac. Sci. Technol., A 15 (1997) 2375–2381.

[4] F. Sharipov, D. Kalempa, Velocity slip and temperature jump coefficients for gaseous mixtures. III: diffusion slip coefficient, Phys. Fluids 16 (2004) 3779–3785.

[5] S. Takata, Diffusion slip for a binary mixture of hard-sphere molecular gases: numerical analysis based on the linearized Boltzmann equation, in: T.J. Bartel, M.A. Gallis (Eds.), Rarefied Gas Dynamics, 22nd International Symposium IP, New York, 2001, pp. 22–29.

[6] H.A. Kramers, J. Kistemaker, On the slip of a diffusing gas mixture along a wall, Physica 10 (1943) 699–713.

[7] T. Graham, On the law of diffusion of gases, Philos. Mag. 2 (1833) 175, 269, 351.

[8] R.Ya. Kucherov, L.E. Rikenglaz, Slipping and temperature discontinuity at the boundary of a gas mixture, Sov. Phys. JETP 36 (1959) 1253–1255.

[9] J. Hoogschagen, Diffusion in porous catalysts and adsorbants, Ind. Eng. Chem. 47 (1955) 906–913.

[10] R.B. Evans, G.M. Watson II, E.A. Mason, Gaseous diffusion in porous media at uniform pressure, J. Chem. Phys. 35 (1961) 2076–2083.

[11] L.B. Rothfield, Gaseous counterdiffusion in catalyst pellets, AIChE J. 9 (1963) 19–24.

[12] R.R. Remick, C.J. Geankoplis, Binary diffusion of gases in capillaries in the transition region between Knudsen and molecular diffusion, Ind. Eng. Chem. Fundam. 12 (1973) 214–220.

[13] E.A. Mason, A.P. Malinauskas, Gas Transport in Porous Media: The Dusty Gas Model, Elsevier, Amsterdam, The Netherlands, 1983.

[14] J.C. Maxwell, On the process of diffusion of two or more kinds of moving particles among one another, Philos. Mag. 20 (1860) 21–38.

[15] S. Whitaker, Mass transport and reaction in catalyst particles, Transp. Porous Media 2 (1987) 269–299.

[16] D.S. Scott, K.E. Cox, Temperature dependence of the binary diffusion coefficient of gases, Can. J. Chem. Eng. 38 (1960) 201–205.

[17] J.B. Young, B. Todd, Modeling of multi-component gas flows in capillaries and porous solids, Int. J. Heat Mass Transfer 48 (2005) 5338–5353.

[18] R.B. Bird, W.E. Stewart, E.N. Lightfoot, Transport Phenomena, second ed., Wiley, New York, 2002.

[19] A.F. Mills, Basic Heat and Mass Transfer, second ed., Prentice Hall, New Jersey, 1999.

[20] J.W. McDonald, V.E. Denny, A.F. Mills, Evaporation and condensation in an enclosure in the presence of a noncondensable gas, in: G.A. Brown, J.R. Moszynski (Eds.), Heat Transfer in Low Reynolds Number Flow, ASME, New York, 1971.

[21] J.P. Meyer, M.D. Kostin, Circulation phenomena in Stefan diffusion, Int. J. Heat Mass Transfer 18 (1975) 1293–1297.

[22] B.L. Markham, F. Rosenberger, Velocity and concentration distributions in a Stefan diffusion tube, Chem. Eng. Commun. 5 (1980) 287–298.

[23] S. Whitaker, Role of species momentum equation in the analysis of the Stefan diffusion tube, Ind. Eng. Chem. Res. 30 (1991) 978–983.

[24] D.E. Rosner, Side-wall gas "creep" and "thermal stress convection" in microgravity experiments on film growth by vapor transport, Phys. Fluids A 1 (1989) 1761–1763.

[25] P.H. Papadopoulos, D.E. Rosner, Direct simulation of concentration creep in a binary gas filled enclosure, Phys. Fluids 8 (1996) 3179–3192.

[26] P.J.A.M. Kerkhof, M.A.M. Geboers, K.J. Ptasinski, On the isothermal transport in a single pore, Chem. Eng. J. 83 (2001) 107–121.

[27] P.J.A.M. Kerkhof, M.A.M. Geboers, Toward a unified theory of isotropic molecular transport phenomena, AIChE J. 51 (2005) 79–121.

[28] P.J.A.M. Kerkhof, M.A.M. Geboers, Analysis and extension of the theory of multicomponent fluid diffusion, Chem. Eng. Sci. 60 (2005) 3129–3167.

[29] A.F. Mills, The use of the diffusion velocity in conservation equations for multicomponent gas mixtures, Int. J. Heat Mass Transfer 41 (1998) 1955–1968.

[30] J.O. Hirschfelder, C.F. Curtiss, R.B. Bird, Molecular Theory of Gases and Liquids, Wiley, New York, 1954.

[31] D.A. Noever, The baroeffect and an appropriate momentum boundary condition, Phys. Fluids A 5 (1990) 858–865.

[32] K.H. Schmitt, Untersuchungen an Schwebstoffteilchen diffundierenden Wasserdamph, Z. Naturforsch. 16a (1961) 144–149.

[33] S.K. Loyalka, Velocity slip coefficient and the diffusion slip velocity for multicomponent gas mixture, Phys. Fluids 14 (1971) 2599–2604.

[34] I.N. Ivchenko, S.F. Loyalka, R.V. Tompson, Boundary slip phenomena in a binary gas mixture, Z. Angew. Math. Phys. 53 (2002) 58–72.

[35] S. Takata, S. Ysuda, S. Kosuge, K. Akoi, Numerical analysis of thermal-slip and diffusion-slip flows of a binary mixture of hard-sphere molecular gases, Phys. Fluids 15 (2003) 3745–3766.

[36] H. Brenner, Navier–Stokes revisited, Physica A 349 (2005) 60–132.

[37] J.R. Bielenberg, The ramifications of diffusive volume transport in classical fluid mechanics, Ph.D. Thesis, Massachusetts Institute of Technology, 2003.

[38] A.F. Mills, Mass Transfer, Prentice-Hall, New Jersey, 2001.

[39] L. Waldmann, K.H. Schmitt, Thermophoresis and diffusiophoresis of aerosols, in: C.N. Davies (Ed.), Aerosol Science, Academic Press, London, 1966.